JAAS FULL PAPER
www.rsc.org/jaas

4009

Elimination of nitric acid interference in ICP-AES by using a cyclonic spray chamber/Nafion membrane-based desolvation system

Antonio Canals,* Luis Gras and Humberto Contreras

Department of Analytical Chemistry, University of Alicante, P.O. Box 99, 03080 Alicante, Spain. E-mail: antonio.canals@ua.es

Received 19th October 2001, Accepted 18th December 2001
First published as an Advance Article on the web 24th January 2002

A vertical cyclonic spray chamber/Nafion membrane-based desolvation system was used to eliminate the nitric acid interference in inductively coupled plasma atomic emission spectroscopy (ICP-AES). Three different matrices were studied: plain water and solutions containing 0.9 and 3.6 mol l^{-1} of nitric acid. The liquid flow rate ranged between 20 and 600 μl min^{-1}. The cyclonic spray chamber was heated at 100 °C and the membrane at 60 °C, using air as dryer gas. The new desolvation system was robust since it accepted a nitric acid concentration change up to 3.6 mol l^{-1} without a change in the emission signal, regardless of the element and line. Hence, elements in these matrices could be calibrated with standards prepared with de-ionized water. In order to test the plasma excitation conditions, the Cr II 267.716 nm to Cr I 357.869 nm line intensity ratio was measured for each combination of desolvation system and matrix. Standard configurations of desolvation systems were also evaluated, and the nitric acid depressive effect could only be eliminated when working at a high spray chamber temperature and/or low liquid flow.

Introduction

Inductively coupled plasma (ICP) is now widely used as a radiation source in atomic emission spectrometry (AES) or as an ionization source in mass spectrometry (MS) for elemental analysis. Both techniques have important advantages (*i.e.*, speed, low limits of detection, various orders of magnitude for calibration graphs, *etc.*) but one of the most significant limitations is the matrix effect. The effect of mineral acids is very common and important.

Inorganic acids are usually present in real samples since they are used for solid sample digestion, liquid sample pretreatment and sample preservation.[1,2] Mineral acid effect has been studied since 1976 and it has been frequently reported that, in ICP-AES, an increase in the acid concentration gives rise to a decrease in the emission signal.[3]

The detrimental effects of mineral acids can be classified into two groups that are physically different: (a) those arising from the processes that happen in the sample introduction system (*i.e.*, nebulizer and spray chamber); and (b) those that take place in the atomizer itself (*i.e.*, plasma or flame). The processes that are in the first group modify the aerosol generation and transport processes because of changes in the sample uptake rate, the aerosol drop size distribution and, hence, analyte transport rate. These changes are mainly due to changes in physical properties of the solution (*i.e.*, viscosity, surface tension and density). The processes produced in the atomizer generate changes in the plasma excitation conditions due to the increased energy consumption for acid atomization and/or a less efficient energy transfer from the coil to the sample.[1,2,4,5] Under hotter or so-called robust plasma conditions and/or an adequate power adjustment, the contribution of the processes that happen in plasma due to acid matrix effect can be reduced or even eliminated. Hence, under these so-called robust plasma conditions the detrimental effect of mineral acids is exclusively due to changes in the processes that take place in the sample introduction system.[6,7]

Methods have been suggested in the literature to minimize the interference of mineral acids. Among them, the most common are: (i) matrix matching; (ii) use of internal standards; (iii) standard additions; and (iv) modification of the sample introduction system.[2,7] In the last case different alternatives have been given: (a) using cyclonic-type spray chambers;[8] (b) using desolvation systems;[4,9] and (c) using direct injection nebulizers.[4,9,10]

The type of spray chamber (*i.e.*, double-pass or cyclonic) is very critical for emission signal reduction induced by the presence of nitric acid.[8,11] When using cyclonic-type spray chambers, the intensity of emission signal suppression by mineral acids depends on the spray chamber material (*i.e.*, glass, polypropylene and polytetrafluoroethylene) and design (*i.e.*, geometry and dimensions), but mainly on the liquid sample uptake rate.[8,11–13] With this spray chamber design the emission signal reduction induced by the presence of nitric acid has been reported to be more pronounced at low liquid flows.[9,10,13,14] Thus, with 1 mol l^{-1} HNO_3 solutions, a signal reduction of 40% was obtained for a liquid flow of 30 μl min^{-1} while the matrix effect was almost eliminated by working at liquid flow rates higher than 80 μl min^{-1}.[10]

Traditionally desolvation systems have been used in atomic spectrometry to reduce the solvent load to the plasma. To this end different designs of desolvation system have been suggested. A typical desolvation system has two main parts: (i) for heating the aerosol; and (ii) for solvent vapor removal from the aerosol stream. The different suggested designs mainly differentiate in the manner of performance of each process. Thus, for solvent evaporation conductive–convective and radiative heating have been used. For solvent vapor removal the most common system is one- or two-step solvent condensation. In some cases membranes have been used in a second step after a cooling step, or as a unique step for solvent elimination.[9,15,16] Membranes have been suggested for desolvation in order to reduce the nucleation process (*i.e.*, condensation of solvent vapor on particle or droplet surfaces) and signal pulses. Nucleation can lead to a loss of analyte resulting in reduction of absolute values of signals, and signal pulsation reduces the signal stability.[17,18] Finally, both effects determine the limits of detection. For this reason the use of membranes can be a good option for aerosol desolvation in atomic spectrometry. At this point, it must be indicated that

DOI: 10.1039/b109562p

two main types of membranes have been used for desolvation: (i) porous and (ii) non-porous. While the former type has been used for both solvent load and acid interference reduction, the latter has only been used for solvent removal.[9,16]

Shen and Chen studied the influence of a desolvation system on the mineral acid interference in ICP-AES with solutions of H_3PO_4 up to 1.5% (w/v). They concluded that when the spray chamber temperature was 240 °C the emission signal obtained with the acid solution was only 5% smaller that with the pure aqueous solution.[19]

Other pioneer work on mineral acid interference elimination by means of membrane-based desolvation systems was presented by Zhu in 1993.[20] In this work the interference effect of 10% of HNO_3 was eliminated by a two-step system for solvent vapor removal, the first one working at −15 °C and the second one being a microporous membrane of PTFE heated at 160 °C. In all these experiments the aerosol was heated at 140 °C.

More recently Todolí *et al.* have practically eliminated the interferences from HNO_3 and H_2SO_4 up to 3.6 mol l^{-1} and 0.9 mol l^{-1}, respectively, working at 30 µl min^{-1} with a spray chamber heating temperature of 160 °C. The solvent vapor was cooled in two steps, the first one at 15 °C and the second one at 0 °C. However, the results were not so good with a membrane-based desolvation system provided with a spray chamber of PTFE heated at 70 °C and a PTFE porous membrane heated at 160 °C. With both desolvation systems the signal reduction with increasing acid concentration still persisted at higher liquid flow rates, which could be partially due to a decrease in the aerosol heating efficiency in the spray chamber.[9]

However, the porous membranes are not specific for the solvent and may cause analyte loss through the permeable membrane material. Nafion is a non-porous ion-exchange material, which allows small polar molecules (*e.g.*, water and to some extent HNO_3) to pass through, while sample particles and non-polar molecules are unaffected. A Nafion dryer operates in a similar fashion to a shell and tube heat exchanger, where two counter-current gas streams transfer heat from one to the other. The big difference is that here moisture is transferred rather than heat. Its polymer backbone is similar to PTFE, making it very resistant to chemical attack. In addition, the Nafion membrane allows air to be used as a sweep gas, in contrast with microporous materials that need argon gas to keep the plasma stable. For this reason, a non-porous Nafion membrane has been suggested as a good alternative to PTFE porous membranes. Until now, Nafion membranes have been exclusively used to reduce the solvent vapor load (*i.e.*, water) in the plasma in ICP-AES, MPT-AES and ICP-MS.[18,21–23] However, to the authors' knowledge, these type of membranes have never been used to eliminate the matrix interference produced by mineral acids in atomic spectrochemical techniques.

Hence, the goal of this work is to evaluate a new desolvation system in order to eliminate nitric acid interference in ICP-AES. The specially designed desolvation system consists of a heated vertical cyclonic spray chamber and a Nafion membrane. With this combination we have tried to eliminate the detrimental effect of nitric acid within the whole desolvation system at low liquid flows and within the cyclonic spray chamber at high liquid flows. In this way all the flow rate values commonly used in ICP-AES will not be influenced by nitric acid.

Experimental

Four desolvation systems were evaluated. In the new design, the aerosols were introduced into a heated all-glass vertical cyclonic spray chamber (VCSC) (volume = 40 ml) followed by a Nafion membrane (M) dryer. Hence, from now on, the overall system will be referred as VCSC-M (Fig. 1(a)). The outlet of the spray chamber was directly connected to the inlet of the membrane. A Tygon drift tube, 1 m in length with 10 mm inner diameter, was used to connect the outlet of the membrane and the inlet of the plasma torch. Three other conventional desolvation systems were used for comparison (Fig. 1(b) and (c)). In all these configurations a single-pass spray chamber (SPSC) was used as a heating step (volume = 110 ml) while different combinations were used for solvent vapor removal. In one of them, two Liebig condensers were connected in series (C-C) (Fig. 1(b)) and in the second one, a Liebig condenser was positioned before the Nafion membrane (C-M) (Fig. 1(c)). The third configuration used for comparison was just the Nafion membrane (M) after the single-pass spray chamber. Hence, the three desolvation systems are refereed to as SPSC-C-C, SPSC-C-M and SPSC-M, respectively.

First of all, the performances of the desolvation systems were optimized. In all these experiments the goals were the analyte transport rate and the solvent removal (*i.e.*, desolvation efficiency). The former must be a maximum while the latter must be a minimum. The manufacturer recommends a membrane temperature of 5 °C lower than the aerosol. Hence, in some experiments, with the membrane as the only solvent removing component, this temperature must be very high (*i.e.*, about 95 °C and 115 °C with the VCSC-M and SPSC-M, respectively). However, if the working temperature of the membrane is very high, the stability of its components deteriorates and also the internal pressure increases. All these factors worsen the performance of the membrane when working at high temperatures. Hence, the selected working temperature of the membrane was a compromise. The optimized experimental conditions obtained for each system are given in Table 1.

The Nafion dryer device contained a Perma Pure dryer (Model PD-625-12-AFS, Tom River, NJ, USA) consisting of 50 strands of Nafion (60 cm long, 0.60 mm id) in a stainless-steel

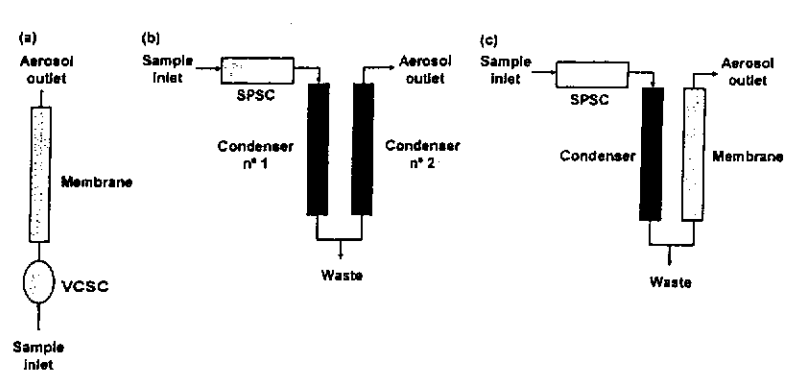

Fig. 1 Schematic diagram of the desolvation systems evaluated. (a) VCSC-M, (b) SPSC-C-C and (c) SPSC-C-M. The fourth desolvation system evaluated (SPSC-M) was a combination of the single-pass spray chamber and the Nafion membrane.

Table 1 Optimized experimental conditions used with the four desolvation systems evaluated

Desolvation system	Temperature/°C				Gas and liquid flows[b]
	Spray chamber	First condenser	Second condenser	Membrane	
SPSC-C-C	120[a]	40	5		Q_g = 0.6 l min^{-1} Q_l = 300 µl min^{-1}
SPSC-C-M	120	40		40	Q_g = 0.6 l min^{-1} Q_l = 300 µl min^{-1} Q_{gm} = 3 l min^{-1}
SPSC-M	120			60	Q_g = 0.6 l min^{-1} Q_l = 300 µl min^{-1} Q_{gm} = 3 l min^{-1}
VCSC-M	100			60	Q_g = 0.6 l min^{-1} Q_l = 600 µl min^{-1} Q_{gm} = 3 l min^{-1}

[a]In some experiments 150 °C. [b]In some experiments Q_l = 20 µl min^{-1}.

cylinder inside a metal box, one side of which was heated to produce a longitudinal temperature gradient. The dryer was sorrounded with a heating tape. The desired heating temperature was set by a temperature controller in contact with the heating tape through a thermistor. Air was driven at 3 l min^{-1}, counter to the aerosol stream direction, through the outside wall of the membrane tube. As the solvent vapor passes through the dryer, a large fraction may be absorbed on the membrane surface and then desorbed by the sweep gas.

The emission signal was measured with a Thermo-Jarrell-Ash sequential ICP-AES instrument (AtomScan Advantage, Franklin, MA, USA). This system is equipped with a 2 kW crystal-controlled rf generator operating at a frequency of 27.12 MHz. The optical system includes a 0.5 m Ebert monochromator equipped with a composite grating of 2400/1200 grooves mm^{-1}. Two photomultiplier detectors were employed, one for the low UV region of the spectrum and the other for the visible-NIR region. Table 2 summarizes the plasma instrumental conditions.

Nitric acid (0.9 mol l^{-1} and 3.6 mol l^{-1}) solutions were the matrices tested. Samples containing seven elements were prepared in plain water or nitric acid solution from a 1000 µg g^{-1} each multielement standard solution (ICP IV, Merck, Darmstadt, Germany). Two analyte concentrations (2.5 and 5.0 µg g^{-1}) were used because of the different sensitivities of the desolvation systems evaluated. Table 3 lists the most relevant properties of the 15 ionic and atomic lines investigated. When the element had more than one line, only the most sensitive line was used to evaluate the precision and limit of detection.

It has been reported that the Mg II/Mg I line intensity ratio is a useful diagnostic tool to evaluate the robustness of the plasma (*i.e.*, the capability of accepting a change in the concentration of the matrix without causing a significant change in the analyte signal).[24–26] However, recently, the Cr II/Cr I line ratio has been suggested as a good alternative for plasma robustness characterization because it is highly sensitive to matrix effects.[7] Hence, this ratio was measured in order to evaluate the plasma excitation conditions obtained with each desolvation system and for each matrix evaluated.

Distribution of solution through the SPSC-C-C desolvation system for each matrix was studied by means of volume measurements of the waste from the spray chamber and condensers. The volume of solution that arrived at the plasma was obtained by difference.

Table 2 Plasma instrumental conditions

Nominal rf power/kW	1.35
Plasma gas flow/l min^{-1}	14
Auxiliary gas flow/l min^{-1}	10
Nebulizer gas flow/l min^{-1}	0.6
Sample uptake rate/ml min^{-1}	Variable (see Table 1)
Nebulizer	Meinhard® TR-30-A3
Torch	Fassel type
Inner diameter of the injector tube/mm	1
Viewing mode	Radial
View distance from coil/mm	15
Integration time/s	2

Results and discussion

The detrimental effect of nitric acid on the analytical signal has been extensively measured in ICP-AES. With the plasma working as a photon source, a 10% signal reduction has been observed for nitric concentrations of 0.9 and 3.9 mol l^{-1} and, in some cases, a reduction of 50% has been measured for an acid concentration between 10% and 30%. In addition to acid concentration, the emission signal suppression has been found to be dependent on the element measured, the energy of the plasma, the sample liquid flow, and the type and dimensions of both the nebulizer and spray chamber used.[1,4,8,11,13,20]

It has been accepted that under robust or hot conditions the energetic plasma conditions are not significantly modified when the sample matrix is changed and, also, an efficient energy transfer exists from the plasma to the sample. Hence, under these conditions, if the anayte signal changes when the matrix concentration is modified, the reason can be attributed to a different part of the instrument (*e.g.*, the sample introduction system).[6] In this work, the plasma instrumental conditions can be considered robust (Table 2). Therefore, the detrimental effect of nitric acid on the emission signal can be exclusively

Table 3 Emission lines tested

Element	λ/nm	E_{sum}[a]/eV
Ca I	422.673	2.94
Cd II	226.502[b]	14.47
Cd I	228.802	5.43
Cr II	267.716[b]	12.92
Cr I	357.869	3.47
Cu II	224.700[b]	15.96
Cu I	324.754	3.83
Cu I	327.396	3.80
Fe II	259.940[b]	12.67
Fe I	248.327	5.01
Fe I	371.994	3.34
Mg II	280.270	12.07
Zn II	206.200	15.4
Zn I	213.856[b]	5.81
Zn I	334.502	7.78

[a]E_{sum} (for ionic lines) = $E_{ionization}$ + $E_{excitation}$; for atomic lines only $E_{excitation}$ is included. [b]Most sensitive line.

attributed to processes that happen during aerosol transport from the nebulizer to the plasma.[27,28]

In addition, it has been reported that ICP-AES is a mass-sensitive detector.[29] This means that the magnitude of the atomic emission signal measured in the plasma should be proportional to the rate of analyte mass delivery to the plasma (*i.e.*, total analyte transport rate).[4,30]

Fig. 2(a) shows the relative net emission intensity (I_{rel} = intensity with HNO_3/intensity without HNO_3) *versus* the energy sum potential (E_{sum}) of the lines studied, obtained with the SPSC-C-C desolvation system and 0.9 mol l^{-1} and 3.6 mol l^{-1} of nitric acid. When I_{rel} reaches a value of unity, it can be said that the matrix effects are negligible. From Fig. 2(a), a clear shift is observed as a function of the acid concentration, while the various patterns remain similar in shape. Secondly, for a fixed acid concentration, no noticeable difference is observed in the net emission signal as a function of the element or line measured. The mean signal reductions are 51 and 75% for the solutions with an acid concentration of 0.9 mol l^{-1} and 3.6 mol l^{-1}, respectively. This is a common trend that has been previously reported for mineral acids in ICP-AES without a desolvation system (*i.e.*, a net emission signal reduction higher for the higher acid concentration, both in radially- and axially-viewed ICP-AES).[9,10,12,28] From these results and from other published results obtained without desolvation, a very important conclusion is that in both plasma viewing modes and with and without a desolvation system, the use of internal standardization can efficiently compensate for nitric acid interference if robust conditions are used.[1,28]

Acid matrix interference has two main contributions from changes in the amount of sample that reaches the plasma and changes in the plasma excitation conditions (or both effects simultaneously). It has been traditionally accepted that, under robust plasma conditions, processes that happen in the plasma can be considered to be constant and, hence, only the processes related to the transport and filtration of the aerosol are acid dependent. In this work, robust conditions and microflow rates for sample uptake were used. Hence, the signal suppression as a function of nitric acid concentration can only be assigned to changes in the aerosol transport from the nebulizer to the plasma. However, recently, some researchers have experimentally proved that even under robust plasma conditions it is not possible to fully suppress a change in plasma conditions. Hence, the depressive effect could still have a contribution attributed to changes in the efficiency of the energy transfer from the plasma to the sample. Traditionally the Mg II/Mg I ratio has been used to study the efficiency of the atomization, excitation and ionization processes in the plasma. The ideal is when no changes are observed in the both the Mg II/Mg I ratio and analyte signal. However, under robust conditions, usually there is no change in the Mg II/Mg I ratio but a change in the analyte signal. This may mean that the plasma conditions have not changed, but the variation in the analyte signal can be explained by problems that arise during aerosol transport and filtration into the spray chamber.[26] Recently, other ionic-to-atomic line intensity ratios have been suggested and evaluated.[7,26,31] Among them the use of the Cr II/Cr I ratio has been suggested, along with adjustment of the incident power in order to maintain the Cr II/Cr I ratio values between standards and samples instead of maintaining the Mg II/Mg I ratio value higher than 8 for radial viewing and a lower value for axial viewing. Chromium ionic-to-atomic line intensity ratio values are given in Table 4 for the four desolvation systems evaluated and the three matrices studied.

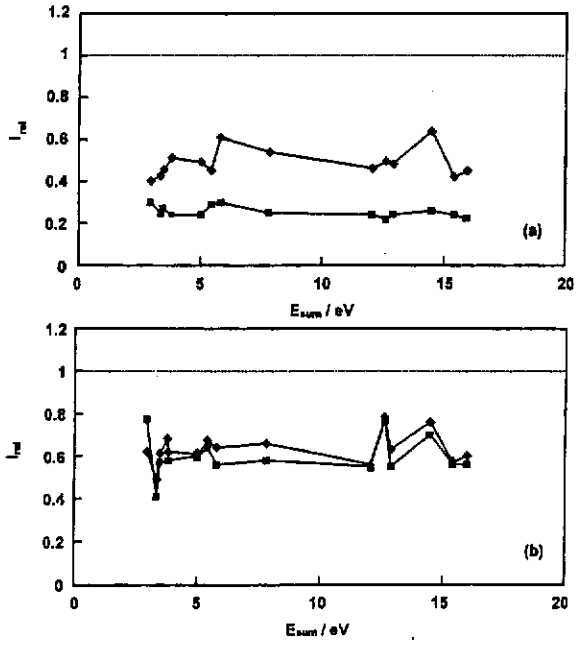

Fig. 2 Relative net emission intensities obtained for: (◆), 0.9 mol l^{-1} HNO_3 and (■), 3.6 mol l^{-1} HNO_3. (a) Desolvation system, SPSC-C-C, (b) desolvation system, SPSC-C-M. T_{sc} = 120 °C; Q_l = 300 µl min^{-1}.

Although the instrumental conditions used in this work can be considered robust, from the ratio values show in Table 4 it may be concluded that, for all the single-pass spray chamber-based desolvation systems evaluated, the energetic plasma conditions change as a function of the matrix nature, and the intensity of these changes depends on the desolvation system used. Thus, with the SPSC-C-C, the chromium ion-to-atom line ratio decreases 20% and 37% for a nitric acid concentration of 0.9 mol l^{-1} and 3.6 mol l^{-1}, respectively. The variation of the ratio values indicates a change in the thermal characteristics of the plasma as a function of matrix type. In order to eliminate, or at least to reduce, this contribution to acid-induced signal suppression, the Cr line ratio values must be made equal among the different matrices and this can be done by power adjustment.[7]

The distribution of the sample nebulized through the desolvation system was also studied in order to evaluate the contribution of the sample introduction system to acid interference. Table 5 shows the distribution of the volume of sample at different points throughout the SPSC-C-C desolvation system for the two acid concentrations evaluated. The sampling points (*i.e.*, SPSC, C-C and P) were the waste outlet of the single-pass spray chamber, the waste outlets of both

Table 4 Chromium ionic-to-atomic line intensity ratio values obtained with the four desolvation systems evaluated

	Cr II/Cr I ratio			
Matrix	SPSC-C-C	SPSC-C-M	SPSC-M	VCSC-M
Plain water	9.3	8.5	6.5	2.9
HNO_3 (0.9 mol l^{-1})	7.4	7.0	4.0	3.0
HNO_3 (3.6 mol l^{-1})	5.9	6.6	4.6	2.7

Table 5 Distribution of volume of solution through the SPSC-C-C desolvation system

Point of sampling[a]	Volume at specified nitric acid concentration (%)	
	0.9 mol l^{-1}	3.6 mol l^{-1}
SPSC	19	32
C-C	70	64
P	11	4

[a]See text for explanation.

condensers and the exit of the second one (*i.e.*, fraction that reaches the plasma).

From the data show in Table 5 it may be seen that the highest sample volume losses were obtained in the condensers (*i.e.*, 70% and 64% for 0.9 mol l^{-1} and 3.6 mol l^{-1} of acid, respectively). In addition, nitric acid has some effect during the aerosol transport from the nebulizer to the plasma. Aerosols with a higher nitric acid concentration would undergo less evaporation and an increase in the droplet density (weight). Also, for acidic aerosols, as the droplets evaporate, the nitric acid concentration is increased, leading to slower evaporation as the drop size becomes smaller. Changes in both analyte and solvent transport rates at the exit of the spray chamber as a function of acid content may be related to the acid-dependent density and aerosol evaporation rate.[1,4] Also, the partial pressure of water vapour depends on the solute and its concentration (*i.e.*, water partial pressure decreases with increasing nitric acid content).[4] Hence, the condensation of solvent vapor in the condensers will be more important with aerosols with a higher nitric acid concentration. The solvent removing process from the aerosol stream into the condenser is mainly due to two processes: (i) condensation on the walls of the condensers and (ii) nucleation on the surface of dry particles and small droplets that exit from the spray chamber. In a simple way, the former process mainly eliminates solvent vapor while the latter process can eliminate both solvent vapor and analyte. As a result of these processes, the net effect at the exit of the desolvation system is a clear reduction in both solvent and analyte transport rates with increasing acid concentration. Thus, a lower amount of solution is introduced into the plasma with a higher acid concentration solution. Nitric acid consumes more energy than water and contributes less to the thermal conductivity of the central channel.[5] Hence, the thermal conditions of the plasma deteriorate as a function of nitric acid concentration (Table 4) and these thermal changes, together with a lower analyte transport rate, can explain the depressive effect of this matrix (Fig. 2(a)). For this discussion it must be accepted that the analyte transport rate values show a variation equal to the variation of volume of solution introduced into the plasma as a function of acid concentration (*i.e.*, lower analyte transport rates with higher acid concentration solutions) (see Fig. 1 of ref. 4).

From previous studies on solvent and analyte transportation through the desolvation systems used in this work, it can be stated that the most significant losses of both solvent and analyte are obtained in the first condenser. Hence, in order to evaluate the performance of the Nafion membrane for removing the remaining solvent vapor (*i.e.*, water and/or nitric acid) from the aerosol stream, the second condenser was substituted by the Nafion membrane.

Fig. 2(b) shows the change in the signal obtained with plain water for the lines evaluated at the two HNO_3 concentrations studied with the SPSC-C-M desolvation system. Two significant conclusions can be obtained from these results. First, a quasi-constant shift can be observed for the whole set of elements. The limiting values of the signal reduction were obtained for Fe I (E_{sum} = 3.34 eV) and Fe II (E_{sum} = 12.67 eV). Secondly, and most important, the signal depression was almost independent of the acid concentration. The signal reduction ranged between 20 and 60% with a mean signal reduction of 38%. Results shown in Fig. 2 indicate that the Nafion membrane was able to reduce the intensity of the interference effect of nitric acid (*i.e.*, from 75% to 38% and from 51% to 38% for the 3.6 mol l^{-1} and 0.9 mol l^{-1} solutions, respectively) and, also, to eliminate the difference between the acidic solutions.

The chromium line ratios obtained with the SPSC-C-M desolvation system and the three matrices used are also shown in Table 4. The values of this ratio were more equal (*i.e.*, ranged between 8.5 and 6.6) than with the SPSC-C-C desolvation system, and the percentage decreases of this ratio, relative to pure water solution, were 18% and 22% for the 0.9 mol l^{-1} and 3.6 mol l^{-1}, respectively. This smaller change in the Cr line ratio values indicates a smaller change in the thermal characteristics of the plasma as a function of acid concentration. However, a small contribution to the change in plasma conditions still remains. Also, the smaller difference in this ratio between both acidic solutions anticipates a similar contribution of the plasma condition changes to the depressive effect. From the results described above, two advantages are obtained with the use of the Nafion membrane: (i) it reduces the signal suppression as a function of nitric acid concentration and (ii) it eliminates the difference in the depressive effect between acid solutions.

The next problem is to find the origin of the 38% signal suppression still remaining with the SPSC-C-M. From the results shown in Table 4 obtained with the SPSC-C-M, it seems that plasma thermal characteristics do not change significantly with the matrix. In addition, from a previous study, it is known that analyte is not lost either in the second condenser or in the membrane. Hence, the remaining signal suppression must mainly originate in the spray chamber or in the first condenser. In order to discern the origin of this remaining signal reduction and the contribution of each one of the components of the sample introduction system, a newly designed desolvation system was constructed and evaluated. This new desolvation system was made with the same single-pass spray chamber and the Nafion membrane (*i.e.*, SPSC-M desolvation system).

The SPSC-M desolvation system shows a similar behavior to the SPSC-C-M (Fig. 2(b)) with changes in nitric acid concentration. With both desolvation systems the severity of signal suppression is not a function of the nitric acid concentration. However, a 17% higher signal reduction (*i.e.*, mean signal reduction approximately 55%) was obtained with the SPSC-M. The main conclusion derived from the results, obtained with the SPSC-C-M and SPSC-M, is that the most significant contribution to the depressive effect of nitric acid originates in the single-pass spray chamber.

Chromium ionic-to-atomic line ratio values obtained with the SPSC-M and the three matrices evaluated are also shown in Table 4. In this case, the thermal characteristics of the plasma were different for the pure water and acidic solutions, being lower for the acidic solutions. Hence, a small contribution to the signal suppresion could still originate in the plasma itself. With this desolvation system all the ratio values were systematically smaller than with the previously evaluated ones. This means that the plasma is less energetic and this could be due to the higher capability of the membrane alone to remove the solvent vapor that exits from the heated spray chamber. As a minimum amount of solvent is needed in order to obtain a good thermal and electrical plasma conductivity,[32] a significant reduction in the total solvent transport rate produces an important diminution of chromium line ratio values.

From the results discussed above it seems that the signal suppression as the nitric acid concentration increases mainly originates in the spray chamber. The signal reduction could be due to changes in the analyte transport rate at the exit of the spray chamber as the result of an inefficient heating of the aerosol. In order to heat efficiently the aerosol entering the spray chamber, different options have been suggested: (i) to increase the spray chamber temperature; (ii) to decrease the sample uptake rate; and (iii) to use a more efficient design of spray chamber (*e.g.*, cyclonic type).[9,32]

The main goal using the three points indicated above is to obtain a more efficient solvent evaporation from the droplets. Hence, the same amount of solution (*i.e.*, analyte) will be transported out of the spray chamber with the three matrices studied.

Fig. 3 shows the results obtained during the evaluation of the

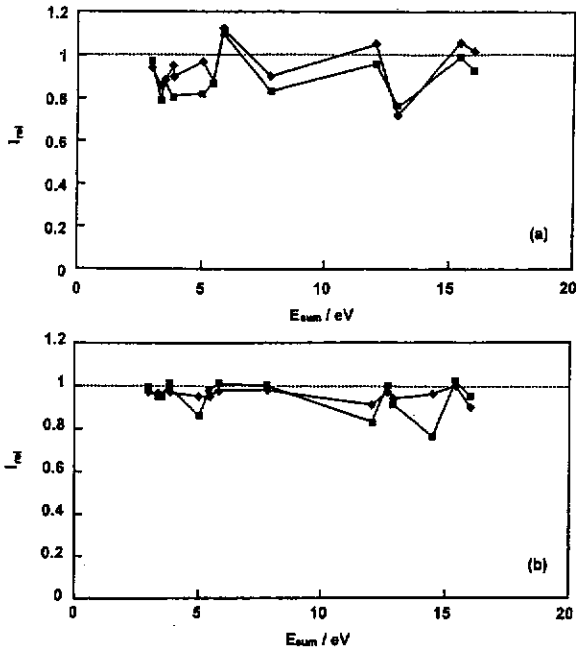

Fig. 3 Relative net emission intensities obtained for: (◆), 0.9 mol l^{-1} HNO_3 and (■), 3.6 mol l^{-1} HNO_3. (a) T_{sc} = 150 °C; Q_l = 300 μl min^{-1}, (b) T_{sc} = 120 °C; Q_l = 20 μl min^{-1}. Desolvation system, SPSC-C-C.

SPSC-C-C desolvation system, with all the lines and the two acid concentrations studied, under a new set of experimental conditions [*i.e*, a higher spray chamber temperature (Fig. 3(a)) and lower sample uptake rate (Fig. 3(b))]. The results shown in Fig. 3(a) were obtained with a temperature in the spray chamber of 150 °C (*i.e.*, an increase of 30 °C relative to the results shown in Fig. 2(a)). Under these conditions the acid effect was significantly reduced compared with using a spray chamber temperature of 120 °C (Fig. 2(a), 51% and 75% mean signal reductions for 0.9 mol l^{-1} and 3.6 mol l^{-1}, respectively). Working with a spray chamber temperature of 150 °C, the mean signal reductions were 6% and 11% for the HNO_3 concentrations of 0.9 mol l^{-1} and 3.6 mol l^{-1}, respectively. Increased emission signals ranging between 5 and 10% were obtained for the Mg II (12.07 eV), Zn II (15.4 eV) and Zn I (5.81 eV) lines at 0.9 mol l^{-1} HNO_3, and for the last atomic line also at 3.6 mol l^{-1} HNO_3.

The emission signals of the elements at the two acid concentrations evaluated obtained with the SPSC-C-C working at 20 μl min^{-1} are shown in Fig. 3(b). A reduction in the sample uptake rate reduces significantly the interference effect of nitric acid. Under these conditions the mean signal suppression was 5%, with a higher signal reduction for Cd II 226.502 nm (24%), Mg II 280.270 nm (17%) and Fe I 248.327 nm (14%), all of them at 3.6 mol l^{-1}. The signal suppression did not appear to be affected greatly by changes in the HNO_3 concentration. Thus, at low liquid flows all the solvent could be absolutely evaporated from the droplets' surfaces and, hence, the analyte transport rate values at the exit of the spray chamber are not a function of acid concentration. In addition, if the sample uptake rate is smaller, the solvent transport rate at the exit of the heated spray chamber will be smaller. Hence, the nucleation process, that mainly happens in the first condenser, will be significantly reduced and consequently the plasma will be more robust. This last conclusion is supported by the relative emission signals of the elements obtained with the SPSC-M at the two acid concentrations studied, working at a sample uptake rate of 20 μl min^{-1}. In this desolvation system, nucleation processes are negligible and the behavior is similar to the desolvation system in which the solvent vapor is eliminated by means of two condensers (Fig. 3(b)). With the SPSC-M, the mean signal suppression is reduced from 55% to 6% when the sample uptake rate is changed from 300 μl min^{-1} to 20 μl min^{-1}, respectively.

Cyclonic type spray chambers are less sensitive to acid effects than the double-pass spray chambers.[8] However, with this type of spray chamber, matrix intereferences still persist when working at low liquid flows in both radially- and axially viewed plasmas.[10–13] A more general solution for the nitric acid interference in emission spectroscopy may be to use a heated cyclonic-type spray chamber.

Fig. 4 shows the corresponding results at the two nitric acid concentrations studied for the VCSC-M desolvation system operated at 600 μl min^{-1} (Fig. 4(a)) and 20 μl min^{-1} (Fig. 4(b)). As expected, the signal depression for both nitric acid concentrations and liquid flows were rather low, differing from unity by no more than ±10% in most cases. This parameter is within the 0.85–1.15 range, with the exception of 0.79 for the Cd II line at 226.502 nm, for a sample uptake rate of 600 μl min^{-1} (Fig. 4(a)), and within the 0.90–1.10 range for the sample uptake rate of 20 μl min^{-1} (Fig. 4(b)). This small emission signal reduction obtained with the VCSC-M for all the elements and lines studied with nitric acid concentration up to 3.6 mol l^{-1} gives a very useful conclusion. With the new desolvation system, particular sample solutions with a nitric acid concentration in the range studied can be directly compared with standards prepared with plain water for a wide range of sample uptake rates (*i.e.*, from 20 μl min^{-1} to 600 μl min^{-1}).

If the results obtained with the SPSC-M, working at T_{sc} = 120 °C and Q_l = 300 μl min^{-1}, and with the VCSC-M, working at T_{sc} = 100 °C and Q_l = 600 μl min^{-1} (Fig. 4(a)), are compared it may be concluded that a significant reduction in the signal suppression is obtained with the heated cyclonic spray chamber at higher liquid flows (*i.e.*, 300 μl min^{-1} and 600 μl min^{-1} for the SPSC and VCSC, respectively) even working at a lower spray chamber temperature (*i.e.*, 120 °C and 100 °C for the SPSC and VCSC, respectively). This means that the cyclonic spray chamber is more efficient for aerosol heating

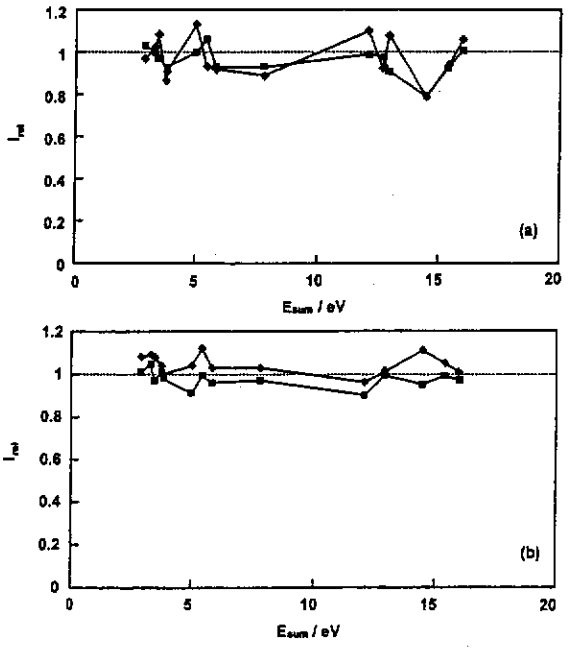

Fig. 4 Relative net emission intensities obtained for: (◆), 0.9 mol l^{-1} HNO_3 and (■), 3.6 mol l^{-1} HNO_3. (a) Q_l = 600 μl min^{-1}, (b) Q_l = 20 μl min^{-1}. Desolvation system, VCSC-M; T_{sc} = 100 °C.

and solvent evaporation than the single-pass one. As has been stated above, one limitation of the cyclonic spray chamber is the elimination of mineral acid effects at low liquid flows. With the VCSC-M this limitation has been removed (Fig. 4(b)) and now this type of spray chamber shows a behavior that is more robust. In this context, the concept of robusness is linked to the capability of the spray chamber to accept a change in the liquid flow rate without a significant change in the relative net emission intensity. For a liquid flow rate of 20 μl min^{-1} the interference ranged between ±10% (Fig. 4(b)).

Among the desolvation systems evaluated, the VCSC-M gives lower chromium ion-to-atom line ratio values (Table 4). Therefore, with this desolvation system, the plasma is cooler than with other desolvation systems. In addition, a smaller range of ratio values among the matrices studied was obtained with this desolvation system. Thus the plasma is more robust in the classical terms of changes in plasma conditions. Hence, if both the sample introduction system and the plasma are robust no interference effect could be anticipated.

From these results, it can be concluded that the more robust VCSC-M desolvation system can cope better with changes in the instrumental conditions than the SPSC-C-C. Nonetheless, the SPSC-C-C gives rise to an increase in the analyte transport rate (*i.e.*, in aqueous solution, 0.8 μg $s^{-1}$and 0.3 μg s^{-1} for the SPSC-C-C and VCSC-M, respectively) and the emission signal values. However, the VCSC-M shows better signal stability than the SPSC-C-C. Both figures of merit finally determine the limits of detection (LOD). Hence, a study of the limits of detection, obtained with both desolvation systems working under optimised instrumental conditions and for the different matrices, is needed.

Relative standard deviation

Relative standard deviation ratios (*i.e.*, $RSD_{SPSC\text{-}C\text{-}C}$/$RSD_{VCSC\text{-}M}$) were obtained for the elements and the three matrices studied. When one element has more than one line available only the most sensitive one (Table 3) was used in this study. The RSD values were obtained under optimized conditions for each desolvation system (Table 1). For all the matrices and elements studied, the RSD values obtained with the SPSC-C-C were, in general, higher than the RSD values obtained with the VCSC-M. In addition, as a general trend, the relative standard deviation ratio values were higher as the acid concentration increased. The better signal stability obtained with the VCSC-M desolvation system could be due to: the lower spray chamber temperature (*i.e.*, 100 °C and 120 °C for the VCSC and SPSC, respectively); and to the damping effect of the membrane, since these systems reduce or even eliminate the plasma pulses produced by the intermittent flash vaporization of droplets that come into contact with the hot walls of the spray chamber and that probably cause pressure variation.[9,18]

Limit of detection

Instrumental limit of detection ratios (*i.e.*, $LOD_{SPSC\text{-}C\text{-}C}$/$LOD_{VCSC\text{-}M}$) for the elements studied, obtained with both desolvation systems as a function of HNO_3 concentration, are given in Fig. 5. In these experiments, only the most sensitive lines were measured. LOD values with the SPSC-C-C and VCSC-M were obtained under the optimized conditions for each desolvation system. With the SPSC-C-C desolvation system, the LOD values ranged between 1.1 ng g^{-1} (Mg in pure water) and 179 ng g^{-1} (Ca in 3.6 mol l^{-1} HNO_3) and, for all the elements studied, an increase in acid concentration deteriorated the LOD values (*i.e.*, LOD values increased). However, this systematic deterioration of LOD values with increasing nitric acid content was not observed with the VCSC-M desolvation system. In addition, the LOD values obtained with the membrane-based system ranged between 0.6 ng g^{-1} (Mg in 0.9 mol l^{-1} HNO_3) and 28.1 ng g^{-1} (Ca in pure water). Limit of detection ratios ranged between 0.7 (Cu in pure water) and 9.7 (Ca in 3.6 mol l^{-1} HNO_3). With the acidic solution the limit of detection values obtained with the VCSC-M were always smaller than the ones obtained with the SPSC-C-C. Hence, the limit of detection ratios changed from 1.0 to 4.5 and from 2.9 to 9.7 for an acid concentration of 0.9 mol l^{-1} and 3.6 mol l^{-1}, respectively. Therefore, the results given in Fig. 5 clearly show the advantage of using a cyclonic spray chamber/Nafion membrane desolvation system, mainly with a high concentration solution of nitric acid. This advantage is a result of the higher heating efficiency of the cyclonic-type spray chamber, the damping effect on the emission signal of the membrane and the lower condensation on the surface of the droplets.

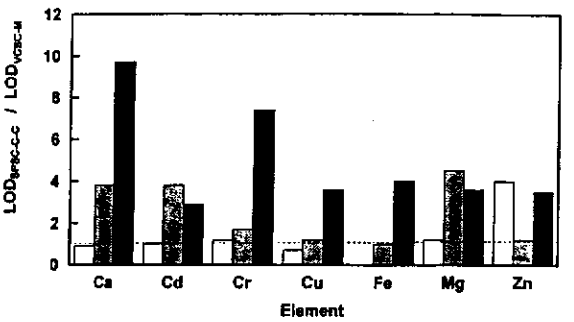

Fig. 5 Limit of detection ratios: (□), plain water; (▨) 0.9 mol l^{-1} HNO_3 and (■), 3.6 mol l^{-1} HNO_3. SPSC-C-C desolvation system: T_{sc} = 120 °C; Q_l = 300 μl min^{-1}. VCSC-M desolvation system: T_{mem} = 60 °C; Q_l = 600 μl min^{-1}. Number of replicates, 20.

Conclusions

The vertical cyclonic spray chamber/Nafion membrane-based desolvation system was able to eliminate completely the depressive effect of nitric acid up to 3.6 mol l^{-1} in ICP-AES for a wide range of sample flow rates (*i.e.*, from 20 μl min^{-1} to 600 μl min^{-1}).

When the new desolvation system is used under robust plasma conditions, different elements and lines could be calibrated with pure aqueous standards.

Other conventional desolvation systems can reduce or eliminate the interference of nitric acid using high spray chamber temperatures and/or low liquid flows.

Finally, and from a practical point of view, the new membrane-based desolvation system evaluated shows some practicalities that must be emphasized. Among them are: (i) less than 1 ml of sample is consumed for a single analysis [*i.e.*, filling the pump tubing and desolvation system, plus the signal(s) adquisition time(s)], including replicates; (ii) the number of samples that can be run per hour is between 10 and 30; and (iii) the membrane shows a very high mechanical and chemical stability. It has been used without any problem for more than three years working with samples of different natures (*e.g.*, aqueous, acidic, organic and high-salt samples). Obviously, some of these characteristics depend on the liquid flow used, number of lines measured and reading mode used (*i.e.*, sequential or simultaneous).

Acknowledgement

The authors wish to thank DGICYT (project number PB95-0693, Spain) for financial support for this work. H.C. also thanks the AECI (Spain) for a fellowship.

References

1 A. Canals, V. Hernandis, J. L. Todolí and R. F. Browner, *Spectrochim. Acta, Part B*, 1995, **50**, 305.
2 J. L. Todolí and J. M. Mermet, *Spectrochim. Acta, Part B*, 1999, **54**, 895.
3 S. Greenfield, H. M. McGeachin and P. B. Smith, *Anal. Chim. Acta*, 1976, **84**, 67.
4 I. I. Stewart and J. W. Olesik, *J. Anal. At. Spectrom.*, 1998, **13**, 1249.
5 I. I. Stewart and J. W. Olesik, *J. Anal. At. Spectrom.*, 1998, **13**, 1313.
6 A. Fernández, M. Murillo, N. Carrión and J. M. Mermet, *J. Anal. At. Spectrom.*, 1994, **9**, 217.
7 E. H. van Veen and M. T. C. de Loos-Vollebregt, *J. Anal. At. Spectrom.*, 1999, **14**, 831.
8 S. Maestre, J. Mora, J. L. Todolí and A. Canals, *J. Anal. At. Spectrom.*, 1999, **14**, 61.
9 J. L. Todolí and J. M. Mermet, *J. Anal. At. Spectrom.*, 1998, **13**, 727.
10 J. L. Todolí and J. M. Mermet, *J. Anal. At. Spectrom.*, 2001, **16**, 514.
11 J. L. Todolí and J. M. Mermet, *J. Anal. At. Spectrom.*, 2000, **15**, 863.
12 J. L. Todolí, S. Maestre, J. Mora, A. Canals and V. Hernandis, *Fresenius' J. Anal. Chem.*, 2000, **368**, 773.
13 M. Catasus, J. L. Todolí, L. Gras and V. Hernandis, *J. Anal. At. Spectrom.*, 2000, **15**, 1203.
14 J. L. Todolí, J. M. Mermet, A. Canals and V. Hernandis, *J. Anal. At. Spectrom.*, 1998, **13**, 55.
15 L. Gras, J. Mora, J. L. Todolí, V. Hernandis and A. Canals, *Spectrochim. Acta, Part B*, 1997, **52**, 1201.
16 Y. Sung and H. B. Lim, *J. Anal. At. Spectrom.*, 2001, **16**, 767.
17 M. A. Tarr, G. Zhu and R. F. Browner, *J. Anal. At. Spectrom.*, 1992, **7**, 813.
18 J. Yang, T. S. Conver, J. A. Koropchak and D. A. Leighty, *Spectrochim. Acta, Part B*, 1996, **51**, 1491.
19 X. E. Shen and Q. L. Chen, *Spectrochim. Acta, Part B*, 1983, **38**, 115.
20 J. J. Zhu, *Elimination of Acid Matrix and Organic Solvent Interferences in Ultrasonic Nebulization ICP-AES*, Oral presentation # 1266, Pittsburgh Conference, Atlanta, GA, USA, 1993.
21 N. Fitzgerald, J. F. Tyson and D. A. Leighty, *J. Anal. At. Spectrom.*, 1998, **13**, 13.
22 E. Debrah and G. Légère, *At. Spectrosc.*, 1999, **20**, 73.
23 Y. Huan, J. Zhou, Z. Peng, Y. Cao, A. Yu, H. Zhang and Q. Jin, *J. Anal. At. Spectrom.*, 2000, **15**, 1409.
24 J. M. Mermet, *Spectrochim. Acta, Part B*, 1989, **44**, 1109.
25 J. M. Mermet, *Anal. Chim. Acta*, 1991, **250**, 85.
26 J. Dennaud, A. Howes, E. Poussel and J. M. Mermet, *Spectrochim. Acta, Part B*, 2001, **56**, 101.
27 J. M. Mermet, *J. Anal. At. Spectrom.*, 1998, **13**, 419.
28 M. Stepan, P. Musil, E. Poussel and J. M. Mermet, *Spectrochim. Acta, Part B*, 2001, **56**, 443.
29 R. F. Browner, A. W. Boorn and D. D. Smith, *Anal. Chem.*, 1982, **54**, 1411.
30 R. F. Browner, A. Canals and V. Hernandis, *Spectrochim. Acta, Part B*, 1992, **47**, 659.
31 J. A. Morales, E. H. van Veen and M. T. C. de Loos-Vollebregt, *Spectrochim. Acta, Part B*, 1998, **53**, 683.
32 J. W. Elgersma, D. T. Thuy and R. P. Groenestein, *J. Anal. At. Spectrom.*, 2000, **15**, 959.